

Responds to the reviewer's comments:

We sincerely thank the reviewer for the valuable comments and suggestions concerning our manuscript entitled "The evolution of cloud microphysics upon aerosol interaction at the summit of Mt. Tai, China". These comments are all valuable and helpful for revising and improving our paper. The responses to reviewers are in blue. The changes are marked in red in the revised manuscript. The Tables and Figures of the revised manuscript were presented at the end of the Responds.

Reviewer 2

General Comments

Comment 1:

The authors present very interesting measurements made at Mt. Tai in northeast China. They have an interesting set of measurements from an under-represented region. As such, it would be valuable for these data to become available. However, I feel that two factors prevent the manuscript from being published in its current form: 1) Substantial revision of the analysis is needed, particularly with regard to the criteria for sub-dividing the cloud events; 2) pertinent references prior to ca. 2000 are lacking, and would perhaps help augment the analysis.

Response: Thank you for your valuable comments. We added descriptions about the criteria for sub-dividing the cloud events in Section 3.2 (Page 8 Line 21 to Page 9 Line 8).

"CP-1 was separated into four stages, including SC1 (stage-clean 1), SP1 (stage-perturbation 1), SC2 (stage-clean 2), and SP2 (stage-perturbation 2) based on whether the perturbation of particles occurred (Fig. 3b). The characteristics of SC1 and SC2 were low N_C (383 \# cm^{-3} and 347 \# cm^{-3} , respectively), large r_{eff} (7.26 \mu m and 6.36 \mu m , respectively) and high LWC/N_C (1.01 ng \#^{-1} and 0.75 ng \#^{-1} , respectively, which represents averaged water each cloud droplet contained) (Fig. 3b). During SP1 and SP2, the perturbation through particles occurred. Dramatic increase of N_C (949 \# cm^{-3} and 847 \# cm^{-3} , respectively) and decrease of r_{eff} (4.90 \mu m and 4.88 \mu m , respectively) and LWC/N_C (0.35 ng \#^{-1} and 0.36 ng \#^{-1} , respectively) was caused.

Each cloud event of CP-2 was separated into activation stage (S1), collision-coalescence stage (S2), stable stage (S3), and dissipation stage (S4) according to the regular changes of N_C and LWC/N_C (Fig. 3a). In S1, N_C dramatically increased to its maximum value among the cloud events. In S2, N_C declined sharply to a stable value, meanwhile LWC/N_C reached the maximum value. In S3, N_C was stable or slightly varied and LWC/N_C started to decrease. In S4, both N_C and LWC/N_C decreased sharply again and finally arrived zero. Even though the two stages (S2 and S3) in CE-25 were not totally follow the division rules, the other six cloud events followed well. It indicated that the division was helpful to study the variations of cloud microphysical properties during CP-2. The newly formed cloud droplets during

S1 were characterized by small size, high N_C and low LWC/N_C values (Fig. 2f and 3b). For example, about 2310 \# cm^{-3} of cloud droplets can quickly form in the first 2 hours of CE-20. The r_{eff} of these droplets was smaller than 4.1 \mu m and LWC/N_C was about 0.2 ng \#^{-1} . In going from S2 to S3, the strong collision-coalescence between cloud droplets caused the increase of both r_{eff} and LWC/N_C . In S4, the increase of $PM_{2.5}$, N_P and T_a (Fig. 2b and Fig. 2c) decreased cloud droplet sizes (Rosenfeld et al., 2014a), decreased the ambient supersaturation, enhanced the evaporation of small droplets (Ackerman et al., 2004), and finally caused the vanishment of cloud events (Mazoyer et al., 2019).”

We cited many useful researches prior to ca. 2000 in the revised manuscript to help us improve our analysis. Such as

Page 2 Line 10 - 16:

“The cloud processes can incorporate large amount of fine particulate mass (Heintzenberg et al., 1989), change the size distributions (Drewnick et al., 2007; Schroder et al., 2015) and alter the CCN compositions through homogeneous and heterogeneous reactions (Roth et al., 2016). In addition, the variation of aerosol number concentrations and size distributions could alter the cloud microphysics. Through studying microphysical characteristics of cloud droplet residuals at Mt. Åreskutan, Noone et al. (1990) found that larger cloud droplets preferred to form on larger Cloud Condensation Nuclei (CCN).”

Page 8 Line 2 - 3:

“Different from convective clouds studied by research aircraft, orographic clouds were mainly formed in the boundary layer as air approaching the ridge, forced to rise up and cooled by adiabatic expansion (Choulaton et al., 1997).”

Page 10 Line 24 – 28:

“What’s more, the perturbation of aerosol particles would cause stronger albedo enhancements when pollution is low in the ambient air (Platnick et al., 2000). Through studying the impact of ship-produced aerosols on the microstructure and albedo of warm marine stratocumulus clouds, Durkee et al. (2000) found that the clean and shallow boundary layers would be more readily perturbed by the addition of ship particle effluents.”

Comment 2:

The grammar and language in the manuscript is understandable, but could be improved.

Response: We improved our grammar and language in the revised manuscript.

Comment 3:

The data are both interesting and useful. However, I feel the manuscript needs

substantial revision before it can be published.

Response: We carefully revised our manuscript based on the comments from the reviewers.

Specific Comments

Comment 1:

P2, L10-15 The processes discussed in this paragraph have been investigated for decades, and there is a very rich literature on all the issues raised. The references here are all fairly recent – which is fine – but I feel that the addition of some citations to earlier studies would help shine a light on how rich the literature on these subjects actually is.

Response: We sincerely thank you for your pertinent comments and valuable suggestions. We cited some valuable papers published before 2000. Such as

Page 2 Line 10 - 16:

“The cloud processes can incorporate large amount of fine particulate mass (Heintzenberg et al., 1989), change the size distributions (Drewnick et al., 2007; Schroder et al., 2015) and alter the CCN compositions through homogeneous and heterogeneous reactions (Roth et al., 2016). In addition, the variation of aerosol number concentrations and size distributions could alter the cloud microphysics. Through studying microphysical characteristics of cloud droplet residuals at Mt. Åreskutan, Noone et al. (1990) found that larger cloud droplets preferred to form on larger Cloud Condensation Nuclei (CCN).”

Page 8 Line 2 - 3:

“Different from convective clouds studied by research aircraft, orographic clouds were mainly formed in the boundary layer as air approaching the ridge, forced to rise up and cooled by adiabatic expansion (Choularton et al., 1997).”

Page 10 Line 24 – 28:

“What’s more, the perturbation of aerosol particles would cause stronger albedo enhancements when pollution is low in the ambient air (Platnick et al., 2000). Through studying the impact of ship-produced aerosols on the microstructure and albedo of warm marine stratocumulus clouds, Durkee et al. (2000) found that the clean and shallow boundary layers would be more readily perturbed by the addition of ship particle effluents.”

Comment 2:

P2, L23 While the “first indirect effect” has become fairly accepted jargon in the cloud physics field, still it should be defined here.

Response: We add the definition of “first indirect effect” in the revised manuscript (Page 1 Line 21 – 22).

“For a given liquid water content, aerosol particles can act as CCN, lead to higher number concentrations

of cloud droplets with smaller sizes and result in higher albedo (Twomey effect or first indirect effect, FIE) (Twomey, 1974).”

Comment 3:

P3, L5 Change “size distributions of clouds and aerosols” to “size distribution of cloud droplets and aerosol particles”.

Response: Thank you. We have revised it in the revised manuscript (Page 3 Line 8 - 9).

“However, lacking knowledge of the size distributions of cloud droplets and aerosol particles makes it difficult to evaluate the cloud microphysics in small-scale regions (Fan et al., 2016;Khain et al., 2015;Sant et al., 2013)”

Comment 4:

P4, entire I feel more detail on data processing is needed. Were inversion routines used to calculate cloud droplet and aerosol particle size distributions and CCN spectra, or were these derived directly from the various instruments?

Response: We added more detailed information about the calibrations of instruments and the corrections of the data in Section 2.2 and Section 2.3 (Page 4 Line 7 to Page 5 Line 28). The CCN spectra was derived directly from the calibrated CCN counter.

“2.2 Cloud microphysical parameters

A Fog Monitor (Model FM-120, Droplet Measurement Technologies Inc., USA), a forward-scattering optical spectrometer with sampling flow of $1 \text{ m}^3 \text{ min}^{-1}$, was applied in situ for real-time displaying size distributions of cloud droplets and computing N_c , LWC, median volume diameter (MVD) and effective diameter (ED) in the size range of 2 to 50 μm (Spiegel et al., 2012). The corresponding equations are:

$$N_c = \sum N_i,$$

$$\text{LWC} = \frac{4\pi}{3} \sum N_i r_i^3 \rho_w,$$

$$\text{MVD} = 2 \times \left(\frac{\sum N_i r_i^3}{\sum N_i} \right)^{\frac{1}{3}}$$

$$\text{ED} = 2 \times r_{eff} = 2 \times \sum n_i r_i^3 / \sum n_i r_i^2,$$

Where N_i is the cloud number concentration at the i th bin, r_i represents the radius at the i th bin and $\rho_w = 1 \text{ g cm}^{-3}$ stands for the density of liquid water. Droplets are categorized into manufacture’s predefined 30 size bins with sampling resolution of 1 s. The size bin widths using this configuration were 1 μm for droplets < 15 μm and 2 μm for droplets > 15 μm . The true air speed calibration and size distribution

calibration of FM-120 were carried out by the manufacturer using borosilicate glass microspheres of various sizes (5.0, 8.0, 15.0, 30.0, 40.0 and 50.0 μm , Duke Scientific Corporation, USA). The difference in optical properties between the glass beads and water was taken into account during the calibration process. In this study, the sampling inlet nozzle faced the main wind direction and was horizontally set. Cloud events are defined by the universally accepted threshold values in N_C and LWC, i.e., $N_C > 10 \text{ \# cm}^{-3}$ and $\text{LWC} > 0.001 \text{ g m}^{-3}$ (Demoz et al., 1996). Too short cloud events with a duration < 15 minutes were excluded.

The topography of the monitoring position could provide the vertical wind field (updraft velocity, v_{up}) and further affect cloud microphysical properties (Verheggen et al., 2007). Based on assumptions that air flow lines were parallel to the terrain and without occurrence of sideways convergence and divergence, v_{up} was estimated by the topography of Mt. Tai and the horizontal wind speed (v_h) measured at the observation station (Hammer et al., 2014), the calculation equation of was:

$$v_{\text{up}} = \tan(\alpha) \times v_h$$

Where α represented the inclination angle which was estimated from the altitudes of Tai'an City and the summit of Mt. Tai and the horizontal distance between them (Fig. S3). It should be noticed that the calculated v_{up} could be considered as the upper limit of the true updraft velocity if the flow lines would not strictly follow the terrain (Hammer et al., 2014). As shown in Table S2, the averaged v_{up} during two focused cloud processes (CP-1 and CP-2) studied in the present study was 1.31 m s^{-1} and 1.07 m s^{-1} , respectively, and did not change a lot. Thus, we simply assumed that the influence of v_{up} on cloud microphysical properties for CP-1 and CP-2 was the same.

In order to estimate the sampling losses due to wind speed and wind direction, the sampling efficiency (contributed by aspiration efficiency and transmission efficiency) was estimated based on the study of Spiegel et al. (2012). The sampling efficiency was depended on two parameters. One is sampling angle (θ_s) which is equal to α . The other is R_V which is equal to the velocity ratio of surrounding wind speed (U_0) with sampling speed (U) of FM-120:

$$R_V = \frac{U_0}{U} = \frac{v_h}{U \cos(\alpha)}$$

In the study of Spiegel et al. (2012), they calculated that the sampling efficiency under standard atmospheric conditions ($p = 1013 \text{ mbar}$, $T = 0 \text{ }^\circ\text{C}$) and represented the results in their Fig. 7. Through calculation, the averaged R_V of CP-1 and CP-2 was 1.04 and 1.16, respectively. Thus, we could use Fig.

7a) from Spiegel et al. (2012), where $R_V = 1.2$, to estimate the sampling efficiency of FM-120 during CP-1 and CP-2. As can be seen, for $\theta_s = \alpha = 11.9^\circ$ and 10.6° (Fig.S3), the aspiration efficiency and transmission efficiency are all close to 1. Thus, we assumed that the influences of topography and updraft velocity on Fog Monitor were small and could be ignored during CP-1 and CP-2.

2.3. Aerosol size distribution

A Scanning Mobility Particle Sizer (SMPS, Model 3938, TSI Inc., USA) consisting of a Differential Mobility Analyzer (DMA, Model 3082, TSI Inc., USA) and a Condensation Particle Counter (CPC, Model 3775, TSI Inc., USA) was applied to monitor the size distributions of dehumidified aerosols through a PM_{10} inlet. The neutralized aerosols were classified by DMA to generate a monodisperse stream of known size according to their electrical mobility. The CPC placed downstream counts the particles and gives the number of particles with different sizes. In the present study, each scan was fixed at 5 min for every loop with a flow rate of 1.5 L min^{-1} sizing particles in the range of 13.6 - 763.5 nm in 110 size bins. The mass concentrations of particles measured by SMPS ($PM_{0.8}$) was calculated from the aerosol number size distribution by simply assuming a density of $\rho = 1.58 \text{ g cm}^{-3}$ (Cross et al., 2007) and compared with the monitored mass concentration of $PM_{2.5}$ (Fig. 2, c). Generally, the variation of $PM_{0.8}$ and $PM_{2.5}$ were highly consistent with each other, especially when $PM_{2.5}$ was less than $20 \mu\text{g m}^{-3}$. In the present study, $PM_{2.5}$ and N_P (the total number concentration of aerosol particles measured by SMPS) were combined together to separate aerosol conditions of cloud processes.”

Comment 5:

P5, L6 “claculated” should be “calculated”

Response: Thank you. We have revised it in the revised manuscript (Page 6 Line 26).

“In the present study, FIE based either on the r_{eff} or on N_C were used calculated as”

Comment 6:

P5, L9 I can't find a definition of N_P , which I assume is total aerosol particle number in the size range the SMPS can measure (13.6-763.5nm). Is this correct?

Response: Yes. We added the definition of N_P in the revised manuscript (Page 5 Line 26 - 28).

“In the present study, $PM_{2.5}$ and N_P (the total number concentration of aerosol particles measured by SMPS) were combined together to separate aerosol conditions of cloud processes.”

Comment 7:

P5, L20-25 The comparisons to cloud conditions at in city fogs, convective and orographic clouds are interesting, but I think comparing to cloud and aerosol measurements at other mountain-top sites would be even better. There are several such sites at which various field campaigns have taken place, with fairly complete aerosol and cloud measurements. These include e.g., Mt. Kleiner Feldberg in Germany, Jungfrauoch in Switzerland, Mt. Åreskutan in Sweden, Puy-de-Dôme in France, Great Dun Fell in the U.K., Mt. Soledad in the US. Some places to start for references to data at these sites are: (recommend papers)

Response: Thank you for your comment. In this part, we want to give an overview of the ranges of the monitored cloud/fog microphysical properties such as N_C , LWC and r_{eff}/MVD . Even though we did not find the corresponding ranges in the the suggested papers, these papers gave abundant observation studies involving size distributions of aerosols and cloud droplets, microphysical and chemical characteristics of cloud droplet residuals/interstitial particles and meteorological and aerosol effects on clouds. We cited them in the revised manuscript to help us comprehensively discuss the aerosol-cloud interactions at Mt. Tai. Such as

Page 2 Line 10 - 16:

“The cloud processes can incorporate large amount of fine particulate mass (Heintzenberg et al., 1989), change the size distributions (Drewnick et al., 2007; Schroder et al., 2015) and alter the CCN compositions through homogeneous and heterogeneous reactions (Roth et al., 2016). In addition, the variation of aerosol number concentrations and size distributions could alter the cloud microphysics. Through studying microphysical characteristics of cloud droplet residuals at Mt. Åreskutan, Noone et al. (1990) found that larger cloud droplets preferred to form on larger Cloud Condensation Nuclei (CCN).”

Page 8 Line 2 - 3:

“Different from convective clouds studied by research aircraft, orographic clouds were mainly formed in the boundary layer as air approaching the ridge, forced to rise up and cooled by adiabatic expansion (Choularton et al., 1997).”

Page 9 Line 14 - 15:

“In contrast, Modini et al. (2015) found negative relation between N_C and the number of particles with diameters larger than 100 nm due to the reduction of supersaturation by coarse primary marine aerosol particles.”

Page 9 Line 30 to Page 10 Line 2:

“In the study of Mazoyer et al. (2019) and Asmi et al. (2012), both of them found that high N_{CCN}/N_P was associated with high κ at a given SS. Thus, $N_{CCN,0.2}$ (N_{CCN} measured at SS = 0.2%) to N_P fractions ($N_{CCN,0.2}/N_P$, CCN activation ratio) is applied to reflect the hygroscopicity of ambient aerosols at Mt. Tai.”

Page 12 Line 3 - 6:

“During CP-2, aerosol particles with diameters larger than 150 nm quickly decreased by activation when

cloud events occurred, while the number of aerosol particles in the size of 50-150 nm were slightly influenced by cloud events (the first panel of Fig. 5a). It was consistent with the study of Targino et al. (2007) who found aerosol size distributions of cloud residuals, which represented aerosol particles activated to cloud droplets, peaked at about 0.15 μm at Mt. Åreskutan.”

Comment 8:

P6, L2-3 I find the discussion here a bit simplistic and even incorrect. LWC often tends to increase linearly with height in a cloud. If entrainment processes are active, the increase of LWC with height could still be linear, but less than the maximum adiabatic rate. Increasing N_c or r_{eff} does not necessarily lead to increases in LWC. You can get an increase in N_c with no increase in LWC by simply having a larger number of smaller droplets. Similarly, r_{eff} can increase at a constant LWC if the droplets became fewer in number but larger in size.

Response: Thank you for your comment. Increasing N_c or r_{eff} does not necessarily lead to increases in LWC. But if LWC increased, it should be influenced by the increase of one of r_{eff} and N_c or both of them. We changed the expression as shown in the revised manuscript (Page 7 Line 24 - 25).

“The increase of LWC should be determined by the increase of r_{eff} and/or N_c .”

Comment 9:

P6, L4 I believe “Hyderaba” should be “Hyderabad”.

Response: Yes. Thank you for your comment. We corrected it in the revised manuscript.

Comment 10:

P6, L13 T_a should be defined before it is used for the first time

Response: We added the definition of T_a in Section 2.5 (Page 6 Line 8 – 10).

“Meteorological parameters including the ambient temperature (T_a , $^{\circ}\text{C}$), relative humidity (RH), wind speed (WS, m s^{-1}) and wind direction (WD, $^{\circ}$) were provided by Shandong Taishan Meteorological Station at the same observation point.”

Comment 11:

P6, L20-30 The sub-periods into which the various cloud events are divided are not clearly defined. What do “clean 1”, “perturbation 2”, “dissipation” and the other descriptors mean?

Response: Based on whether the perturbation of particles occurred, CP-1 was divided into four stages. Compared with two clean stages (SC1 and SC2), two stages with perturbation of aerosol particles (SP1 and SP2) were characterized with higher N_c , smaller r_{eff} and lower LWC/N_c . The averaged characteristic values of N_c , r_{eff} and LWC/N_c during SP1, SP2, SC1 and SC2 were

added in the revised manuscript. According to the regular changes of N_C and LWC/N_C , each cloud event of CP-2 was divided into four stages. The variation of N_C during the four stages was described in the Page 8 Line 21 to Page 9 Line 8.

“CP-1 was separated into four stages, including SC1 (stage-clean 1), SP1 (stage-perturbation 1), SC2 (stage-clean 2), and SP2 (stage-perturbation 2) based on whether the perturbation of particles occurred (Fig. 3b). The characteristics of SC1 and SC2 were low N_C (383 \# cm^{-3} and 347 \# cm^{-3} , respectively), large r_{eff} (7.26 \mu m and 6.36 \mu m , respectively) and high LWC/N_C (1.01 ng \#^{-1} and 0.75 ng \#^{-1} , respectively, which represents averaged water each cloud droplet contained) (Fig. 3b). During SP1 and SP2, the perturbation through particles occurred. Dramatic increase of N_C (949 \# cm^{-3} and 847 \# cm^{-3} , respectively) and decrease of r_{eff} (4.90 \mu m and 4.88 \mu m , respectively) and LWC/N_C (0.35 ng \#^{-1} and 0.36 ng \#^{-1} , respectively) was caused.

Each cloud event of CP-2 was separated into activation stage (S1), collision-coalescence stage (S2), stable stage (S3), and dissipation stage (S4) according to the regular changes of N_C and LWC/N_C (Fig. 3a). In S1, N_C dramatically increased to its maximum value among the cloud events. In S2, N_C declined sharply to a stable value, meanwhile LWC/N_C reached the maximum value. In S3, N_C was stable or slightly varied and LWC/N_C started to decrease. In S4, both N_C and LWC/N_C decreased sharply again and finally arrived zero. Even though the two stages (S2 and S3) in CE-25 were not totally follow the division rules, the other six cloud events followed well. It indicated that the division was helpful to study the variations of cloud microphysical properties during CP-2. The newly formed cloud droplets during S1 were characterized by small size, high N_C and low LWC/N_C values (Fig. 2f and 3b). For example, about 2310 \# cm^{-3} of cloud droplets can quickly form in the first 2 hours of CE-20. The r_{eff} of these droplets was smaller than 4.1 \mu m and LWC/N_C was about 0.2 ng \#^{-1} . In going from S2 to S3, the strong collision-coalescence between cloud droplets caused the increase of both r_{eff} and LWC/N_C . In S4, the increase of $PM_{2.5}$, N_P and T_a (Fig. 2b and Fig. 2c) decreased cloud droplet sizes (Rosenfeld et al., 2014a), decreased the ambient supersaturation, enhanced the evaporation of small droplets (Ackerman et al., 2004), and finally caused the vanishment of cloud events (Mazoyer et al., 2019).”

Comment 12:

P6, L23 The authors divide liquid water content by cloud droplet number concentration (LWC/N_C) and report a value of 1.9 mg water per droplet. This is clearly erroneous. For a water density of 1 g cm^{-3} , this would give a droplet radius of 0.8mm, which is clearly far too large. This comment holds true for Figure 3(b) as well.

Response: Thank you for your comment. We checked our data and found that we misused the unit of N_C when we calculated the values of LWC/N_C . The unit of N_C should be $\# \text{ cm}^{-3}$ instead of $\# \text{ m}^{-3}$. Thus, the result was overestimated with a factor of 10^6 . The number is correct but the unit should be $\text{ng} \#^{-1}$ for LWC/N_C . We have corrected the corresponding units in the text and in Fig. 3(b). (Page 8 Line 22 - 26)

“The characteristics of SC1 and SC2 were low N_C ($383 \# \text{ cm}^{-3}$ and $347 \# \text{ cm}^{-3}$, respectively), large r_{eff} ($7.26 \mu\text{m}$ and $6.36 \mu\text{m}$, respectively) and high LWC/N_C ($1.01 \text{ ng} \#^{-1}$ and $0.75 \text{ ng} \#^{-1}$, respectively, which represents averaged water each cloud droplet contained) (Fig. 3b). During SP1 and SP2, the perturbation through particles occurred. Dramatic increase of N_C ($949 \# \text{ cm}^{-3}$ and $847 \# \text{ cm}^{-3}$, respectively) and decrease of r_{eff} ($4.90 \mu\text{m}$ and $4.88 \mu\text{m}$, respectively) and LWC/N_C ($0.35 \text{ ng} \#^{-1}$ and $0.36 \text{ ng} \#^{-1}$, respectively) was caused.”

Comment 13:

P7, L11-13 The bounding lines referred to here (and shown in Figure 3(d)) appear arbitrary. Is there any physical explanation for these lines? Why does one have a zero intercept and the other an intercept of -200?

Response: Due to the limitation of instruments, we could not directly get the hygroscopicity parameter κ . In the study of Asmi et al. (2012), they conducted the study at Puy-de-Dome and discussed the relations between the number concentration of CCN, the number concentration of aerosol particles and the hygroscopicity parameter κ . The two dashed linear lines represented the visually defined boundaries in within most of the data at Puy-de-Dome are centered. We cited these two lines and wanted to compare their data with ours. We found that most of our data was also centered between these two dashed lines. Asmi et al. (2012) found that a good linear fit of CCN versus N_P and higher values of κ existed in winter. The data of CP-2 (Figure 3d) at Mt. Tai was similar with the winter data at Puy-de-Dome that good linear fits of CCN versus N_P existed. Thus, we speculated that the values of κ of CP-2 might be higher than that of CP-1. We rephrased the corresponding part in the revised manuscript in Page 9 Line 29 to Page 10 Line 10.

“The hygroscopicity of aerosols determines the ability of aerosols acted as CCN, which can further influence cloud number concentrations. Due to the lack of corresponding instruments, the hygroscopicity parameter κ is not available. In the study of Mazoyer et al. (2019) and Asmi et al. (2012), both of them found that high N_{CCN}/N_P was associated with high κ at a given SS. Thus, $N_{\text{CCN},0.2}$ (N_{CCN} measured at SS = 0.2%) to N_P fractions ($N_{\text{CCN},0.2}/N_P$, CCN activation ratio) is applied to reflect the hygroscopicity of ambient aerosols at Mt. Tai. As shown in Fig. 3b $N_{\text{CCN},0.2}/N_P$ ranged from 0.06 to 0.69 in CP-1 yet it was range from 0.22 to 0.66 in CP-2. The plot of $N_{\text{CCN},0.2}$ versus N_P was more scatter in CP-1 than that in CP-2 (Fig. 3b and Fig. 3c). Values lower than 0.22 did not appear during CP-2. Even though the settled SS

in the present study ($SS = 0.2\%$) is different from that at Puy-de-Dôme ($SS = 0.24\%$), most of the data points of CP-1 and CP-2 were distributed between the two recommended dashed lines (the visually defined boundaries in which most of the data are centered, Fig. 3c and 3d) by Asmi et al. (2012). During the observation program at Puy-de-Dôme, France, Asmi et al. (2012) found that higher N_{CCN}/N_P and more concentrated plots of $N_{CCN,0.2}$ versus N_P were usually observed during winter when higher fractions of aged organics were observed. It indicated that the difference of aerosol organic chemical compositions during CP-1 and CP-2 might influence the κ of aerosols and further affect the N_{CCN}/N_P ratio during these two cloud processes.”

Comment 14:

P8, L1-13 Once again, references seem to be limited to rather recent publications. There is a wealth of literature about cloud susceptibility starting in the 1990s. I suggest starting with [Platnick, S., P. A. Durkee, K. Nielsen, J. P. Taylor, S. C. Tsay, M. D. King, R. J. Ferek, P. V. Hobbs, and J. W. Rottman (2000), The role of background cloud microphysics in the radiative formation of ship tracks, *J Atmos Sci*, 57(16), 2607-2624] and the papers that cite this one for more comparisons.

Response: Thank you for your suggestions. The papers recommended by the reviewer give information on the sensitivity of clouds to changes in aerosol particles. They are helpful to augment discussion in Section 3.2.2. We cited the studies of Platnick et al., (2000) and Durkee et al. (2000) in Section 3.2.2 (Page 10 Line 24 - 28).

“What’s more, the perturbation of aerosol particles would cause stronger albedo enhancements when pollution is low in the ambient air (Platnick et al., 2000). Through studying the impact of ship-produced aerosols on the microstructure and albedo of warm marine stratocumulus clouds, Durkee et al. (2000) found that the clean and shallow boundary layers would be more readily perturbed by the addition of ship particle effluents.”

Comment 15:

P8, L18 I have a difficult time understanding how soluble organic particles can be hydrophobic.

Response: Thank you for your careful review. The SSO should be “slightly soluble organics” Yuan et al., (2008). We made corrections in the revised manuscript. (Page 11 Line 10 - 13)

“By using the 2-D Goddard Cumulus Ensemble model (GCE), Yuan et al. (2008) explained that the positive relationship between r_{eff} and AOD appeared to originate from the increasing slightly soluble organics (SSO) particles. The increase of SSO would act to increase the critical supersaturation for

particles to be activated and resulted in less numbers of activated particles.”

Comment 16:

P8, L28+ The discussion of Figure 5 is confusing, mostly because the figure itself is not clearly labeled. There is a great deal of information in Fig. 5; at a minimum, a clear caption is necessary. I’m afraid I can’t follow the arguments presented here, and feel this material needs significant work to be understandable.

Response: We added detailed captions in the revised manuscript. (Page 11 Line 22 to Page 12 Line 9)

“3.2.3 Size distribution of cloud droplets and particles

To illustrate the evolution of the aerosol particles and the cloud droplets during the cloud processes, the size distributions of N_p and N_c during different cloud stages are plotted in Fig. 5. For each of the four size bins ranged from 2 to 13 μm , cloud number concentrations of SC1 and SC2 were lower than those of SP1 and SP2. In the size bin of 13–50 μm , however, N_c of SC1 and SC2 were the largest (Fig. 5b). This size distributions of cloud droplets in SC1 and SC2 resulted in the larger r_{eff} during the two stages, which was consistent with the result shown in Fig. 3b. During two perturbation stages of SP1 and SP2 in CP-1, the numbers of aerosol particles in all size bins increased. But the increase of aerosol particles larger than 150 nm was the smallest, indicating that aerosols larger than 150 nm were more easily activated into cloud droplets. The activation of aerosol particles with the size larger than 150 nm in the present study dramatically increased N_c of 5–10 μm and made N_c of SP1 and SP2 in different size bins all comparable with those of CP-2 (Fig. 5b).

As shown in Fig. 5c, cloud droplets with D_c ranging from 5 to 10 μm had high N_c in each stage in CP-2 and cloud droplets with D_c ranging from 13 to 50 μm had low N_c in each stage if compared to CP-1. It caused the lower r_{eff} in CP-2 than CP-1. During CP-2, aerosol particles with diameters larger than 150 nm quickly decreased by activation when cloud events occurred, while the number of aerosol particles in the size of 50-150 nm were slightly influenced by cloud events (the first panel of Fig. 5a). It was consistent with the study of Targino et al. (2007) who found aerosol size distributions of cloud residuals, which represented aerosol particles activated to cloud droplets, peaked at about 0.15 μm at Mt. Åreskutan. Mertes et al. (2005) also found that particles centered at $d_p = 200$ nm could be efficiently activated to droplets while most Aitken mode particles remained in the interstitial phase. Compared with other stages, S1 had the highest N_c in three size bins of [2, 5) μm and [5, 7) μm . It indicated that large numbers of cloud droplets with small sizes were formed in the beginning of cloud events in CP-2.”

Comment 17:

P9, L19 Given the amount of temporal variability in LWC, do hourly averages of this quantity have any real meaning?

Response: The time resolution of the corresponding data in Figure 6(a) should be 5 min. We have corrected it in the revised manuscript (Page 12 Line 11 – 12). As shown in Figure R1, the relations between LWC and r_{eff} were consistent even though data with different time resolutions (1 min and 5 min) were applied. In order to make the picture clearer, we choose the 5 min averaged data to plot Figure 6(a). However, the data in Figure 6(c) was 50 min averaged, which was depended on the time resolution of CCN. We added the description of time resolutions we applied in the figure caption.

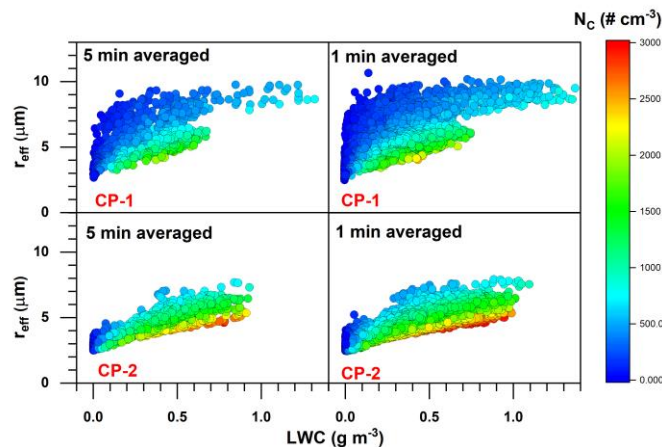


Figure R1. The plot of LWC versus r_{eff} of CP-1 and CP-2. Time resolutions of the corresponding data were 5 min and 1 min, respectively.

“The 5 min averaged LWC for CP-1 and CP-2 is plotted against corresponding r_{eff} in Fig. 6a. Large cloud droplets ($r_{\text{eff}} > 8 \mu\text{m}$) were observed in CP-1, while the r_{eff} for CP-2 varied narrowly in the range of 2.5–8 μm .”

Comment 18:

P9, L26-27 As per my previous comments, I feel that the stages into which the authors divide cloud period 2 are arbitrary. I haven’t found any explanation of these stages in terms of quantitative parameters. The physical processes discussed on pages 9-10 are certainly valid ones, and pertain to clouds in general. However, I don’t find the division of the cloud events into arbitrary stages to be convincing in terms interpreting the measurements at Mt. Tai in the context of these processes. Unfortunately, I feel that Figure 6 and the discussion around it is unconvincing. There may well be interesting information here, but a clearer rationale for stratification of the data will be necessary before it can be elucidated.

Response: During each cloud event of CP-2, the variations of N_c and LWC/N_c were applied to divide different stages of cloud events. The corresponding rules were detailedly described in Page 8 Line 27 to Page 9 Line 8.

“Each cloud event of CP-2 was separated into activation stage (S1), collision-coalescence stage (S2), stable stage (S3), and dissipation stage (S4) according to the regular changes of N_C and LWC/N_C (Fig. 3a). In S1, N_C dramatically increased to its maximum value among the cloud events. In S2, N_C declined sharply to a stable value, meanwhile LWC/N_C reached the maximum value. In S3, N_C was stable or slightly varied and LWC/N_C started to decrease. In S4, both N_C and LWC/N_C decreased sharply again and finally arrived zero. Even though the two stages (S2 and S3) in CE-25 were not totally follow the division rules, the other six cloud events followed well. It indicated that the division was helpful to study the variations of cloud microphysical properties during CP-2. The newly formed cloud droplets during S1 were characterized by small size, high N_C and low LWC/N_C values (Fig. 2f and 3b). For example, about 2310 \# cm^{-3} of cloud droplets can quickly form in the first 2 hours of CE-20. The r_{eff} of these droplets was smaller than 4.1 \mu m and LWC/N_C was about 0.2 ng \#^{-1} . In going from S2 to S3, the strong collision-coalescence between cloud droplets caused the increase of both r_{eff} and LWC/N_C . In S4, the increase of $PM_{2.5}$, N_P and T_a (Fig. 2b and Fig. 2c) decreased cloud droplet sizes (Rosenfeld et al., 2014a), decreased the ambient supersaturation, enhanced the evaporation of small droplets (Ackerman et al., 2004), and finally caused the vanishment of cloud events (Mazoyer et al., 2019).”

We revised our discussion about Figure 6 in Page 12 Line 10 to Page 13 Line 24.

“3.3. Relations among LWC, r_{eff} and N_C

The 5 min averaged LWC for CP-1 and CP-2 is plotted against corresponding r_{eff} in Fig. 6a. Large cloud droplets ($r_{\text{eff}} > 8 \text{ \mu m}$) were observed in CP-1, while the r_{eff} for CP-2 varied narrowly in the range of 2.5–8 μm .

Cloud droplets with $r_{\text{eff}} > 8 \text{ \mu m}$ only occurred in the two relatively clean stages, SC1 and SC2, during CP-1. It was due to the weaker competition among droplets at lower N_{CCN} conditions. This has also been observed in the U.S. Mid-Atlantic region where cloud droplets with larger sizes are more easily formed with lower N_{CCN} (Li et al., 2017b). At the same LWC level, the growth of cloud droplets during SP1 and SP2 was obviously limited if compared with SC1 and SC2, which is referred to as the “Twomey effect” (Twomey, 1977). This is consistent with the illustration in Fig. 3 that cloud droplets in SP1 and SP2 were smaller.

The variation of LWC was determined by the change of r_{eff} and/or N_C . However, the decisive factor may be different in different stages of the cloud. As shown in the lower panel of Fig. 6a, CE-20 was taken

as an example to discuss the relation among LWC, R_{eff} and N_C in different cloud stages. During S1, the existing numerous CCN (Fig. 3a) were quickly activated to form cloud droplets. The newly formed droplets are characterized with small sizes but large numbers. They will suppress the beginning of collision-coalescence processes (Rosenfeld et al., 2014a) and may further significantly delay raindrop formation Qian et al. (2009). In S1, positive relation existed between N_C and r_{eff} . Both the increase in N_C (from 1188 \# cm^{-3} to 2940 \# cm^{-3}) and the growth of r_{eff} (from $\sim 3.5 \text{ \mu m}$ to $\sim 4.5 \text{ \mu m}$) boosted the LWC in this stage. This is different from Mazoyer et al. (2019)'s result that they found a clearly inverse relationship between the number and the size of droplets at the beginning of the first hour of fog events during the observation in suburban Paris. When compared with fog, cloud is usually formed under conditions with more condensible water vapour (Fig. 1). The limited growth of droplets in fog will not occur in cloud. It caused the positive relationship with cloud droplet number and droplet size. At the beginning of S2, N_C reaches the maximum. The high N_C yields a great coalescence rate between cloud droplets. Meanwhile, the coalescence process is self-accelerating (Freud and Rosenfeld, 2012) and thus causes the quick decrease of N_C (Fig. 3a). This makes cloud droplets in S2 characterized by larger sizes as well as lower number concentrations, whilst LWC simply varies in a relatively narrow range (Fig. 6a). During S3, N_C is almost constant due to the formation, coagulation, and evaporation of the cloud droplets reaching a balance. As shown in the panel, the relationship between r_{eff} and LWC in this stage could be fitting as $r_{\text{eff}}=a \times \text{LWC}^{0.34 \pm 0.02}$, which means under the increase of LWC, the N_C was almost unchanged. The variation of LWC values is mainly due to the changes of droplet sizes. At the dissipation stage of S4, the clouds vanish due to mixing with the dry ambient air (Rosenfeld et al., 2014a). The previously activated CCN returned back to the interstitial aerosol phase due to the evaporation of the droplets (Verheggen et al., 2007). Both N_C and r_{eff} decline. It also illustrates in Fig. 5c that all the N_C of the five size bins of cloud droplets decrease in S4.

In order to investigate the variation of r_{eff} upon N_C , the distribution of r_{eff} was classified with different N_C ranges in Fig. 6b. For $N_C < 1000 \text{ \# cm}^{-3}$, r_{eff} displayed a trimodal distribution and concentrated on 3.25 \mu m (Peak-1), 4.86 \mu m (Peak-2) and 7.52 \mu m (Peak-3), respectively. Peak-1 corresponded to cloud droplets with low N_C , LWC, and r_{eff} values while the $N_{\text{CCN}0.2}$ was very high (Fig. 6c). These points represented cloud droplets in the incipient stage or the dissipation stage of cloud events where large numbers of CCN exist in the atmosphere. Peak-2 and Peak-3 represented the mature stages for cloud events with different environmental conditions. Peak-3 represented cloud droplets formed

under a relatively cleaner atmosphere. In this circumstance, CCN were efficiently activated and had a lower concentration remaining in the atmosphere (Fig. 6c). The sufficient ambient water vapour accelerated the growth of the formed droplets, which were characterized with low N_C and LWC but large r_{eff} . Peak-2 represented cloud droplets formed under relatively polluted conditions and was the only peak found for N_C larger than 1000 \# cm^{-3} . With the increase of N_C , the distribution of this peak narrowed and slightly moved to lower r_{eff} mode.

The thickness of orographic cloud was usually very thin (Welch et al., 2008). If assuming the cloud thickness during CP-1 and CP-2 were equal, albedo would depend on the values of LWC and N_C as described in Section 2.8. Cloud albedo during CP-2 was always higher than that during CP-1, especially when the cloud thickness was lower than about 2500 m (Fig. 6d). Through studying marine stratocumulus clouds in the north-eastern Pacific Ocean, Twohy et al. (2005) also found that the increase of N_C by a factor of 2.8 would lead to 40% increase of albedo going from 0.325 to 0.458. It indicated that the higher N_C would increase the cloud albedo if assuming no change of cloud thickness.”

Comment 19:

P10, L27 Is there any reason to assume that the cloud thickness is 100m? My own experience measuring clouds from mountaintop sites is that cloud thickness varies quite dramatically, and at most sites is highly sensitive to changes in wind speed and direction.

Response: Based on the equations in Section 2.8, albedo depends on the values of LWC, N_C and cloud thickness. Here, we set the same cloud thickness for CP-1 and CP-2, and discuss the difference between albedo due to the change of LWC and N_C . Unfortunately, we don't have the corresponding data of cloud thickness during our monitoring program. In the revised manuscript, we applied the averaged values of LWC and N_C of CP-1 and CP-2 to calculate the corresponding albedo during CP-1 and CP-2. For a given cloud thickness, albedo during CP-2 was always higher than that during CP-1 if the cloud thickness is lower than about 2500 m (Fig. 6d). We revised this part in Page 13 Line 19 - Line 24.

“The thickness of orographic cloud was usually very thin (Welch et al., 2008). If assuming the cloud thickness during CP-1 and CP-2 were equal, albedo would depend on the values of LWC and N_C as described in Section 2.8. Cloud albedo during CP-2 was always higher than that during CP-1, especially when the cloud thickness was lower than about 2500 m (Fig. 6d). Through studying marine stratocumulus clouds in the north-eastern Pacific Ocean, Twohy et al. (2005) also found that the increase of N_C by a factor of 2.8 would lead to 40% increase of albedo going from 0.325 to 0.458. It indicated that the higher N_C would increase the cloud albedo if assuming no change of cloud thickness.”

Comment 20:

Figure 2 The rightmost label in panel (e) of Figure 2 $dN/d\log D_c$, not $dN/d\log D_p$

Response: Thank you for your comment. We have corrected the label in the revised manuscript.

Comment 21:

Figure 5 This figure is very colorful, but very difficult to understand. The figure caption needs significantly more detail.

Response: We added detailed captions in the revised manuscript.

Tables and Figures

Table 1: Comparison of clouds monitored at Mt. Tai with city fogs, convective clouds monitored by research aircrafts and other orographic clouds. Including sampling information (site, period and altitude), the range of PM_{2.5} mass concentrations, the range of microphysical parameters (number concentrations of cloud droplets-N_c, liquid water content-LWC, median volume diameter-MVD, effective radius-r_{eff}) and the number of monitored clouds/cloud events/fog events.

Sampling Site	Period	Altitude (m a.s.l)	PM _{2.5} ($\mu\text{g m}^{-3}$)	N _c (# cm ⁻³)	LWC (g m ⁻³)	MVD (μm)	r _{eff} (μm)	Number of clouds/cloud events/fog events	Reference
City Fog									
Shanghai, China	Nov. 2009	7	-	11-565	0.01-0.14	5.0-20.0	-	1	(Li et al., 2011)
Nanjing, China	Dec. 2006- Dec. 2007	22	0.03 ^a -0.60 ^a	-	2.69e ⁻³ -0.16	-	1.6 ^b -2.7 ^b	7	(Lu et al., 2010)
Convective Clouds									
Amazon Basin/cerrado reCompagions, Brazil	Aug.-Sept. 1995	90-4000	-	-	0 ^d -2.10 ^d	-	2.8 ^d -9.2 ^d	>1000	(Reid et al., 1999)
Hyderabad - The Bay of Bengal, India	29 th Oct. 2010	1300- 6300	-	10 ^d -380	0 ^d -1.80	-	3.8 ^d -17.0	1	(Padmakumari et al., 2017)
Orographic clouds									
Mt. Schmöcke, Germany	Sep.-Oct. 2010	937	-	-	0.14-0.37	-	5.7-8.7	8	(Van Pinxteren et al., 2016)
East Peak Mountain, Puerto Rico	Dec. 2004	1040	-	193-519	0.24-0.31	14.0-20.0	-	2	(Allan et al., 2008)
Mt. Tai, China	Jul.-Aug. 2014	1545	11.1-173.3	4-2186	0.01-1.52	1.6-43.0	0.8-18.9	24	Unpublished data from (Li et al., 2017a)
Mt. Tai, China	Jun.-Jul. 2018	1545	1.2-127.1	10-3163	1.01e ⁻³ -1.47	4.4-25.0	2.4-13.4	40	This study
Mt. Tai, China (CP-1 ^c)	10 th – 13 th Jul. 2018	1545	1.3-40.7	11-2470	1.12e ⁻³ -1.47	4.6-17.4	2.5-10.7	12	This study
Mt. Tai, China (CP-2 ^c)	13 th – 20 th Jul. 2018	1545	1.2-66.2	10-3163	1.03e ⁻³ -1.10	4.6-13.5	2.4-7.9	12	This study

^a Represents the mass concentrations of PM₁₀. ^b Represents the range of averaged radius. ^c Two cloud processes which are detailedly discussed in this study. ^d Values were read from the graphs.

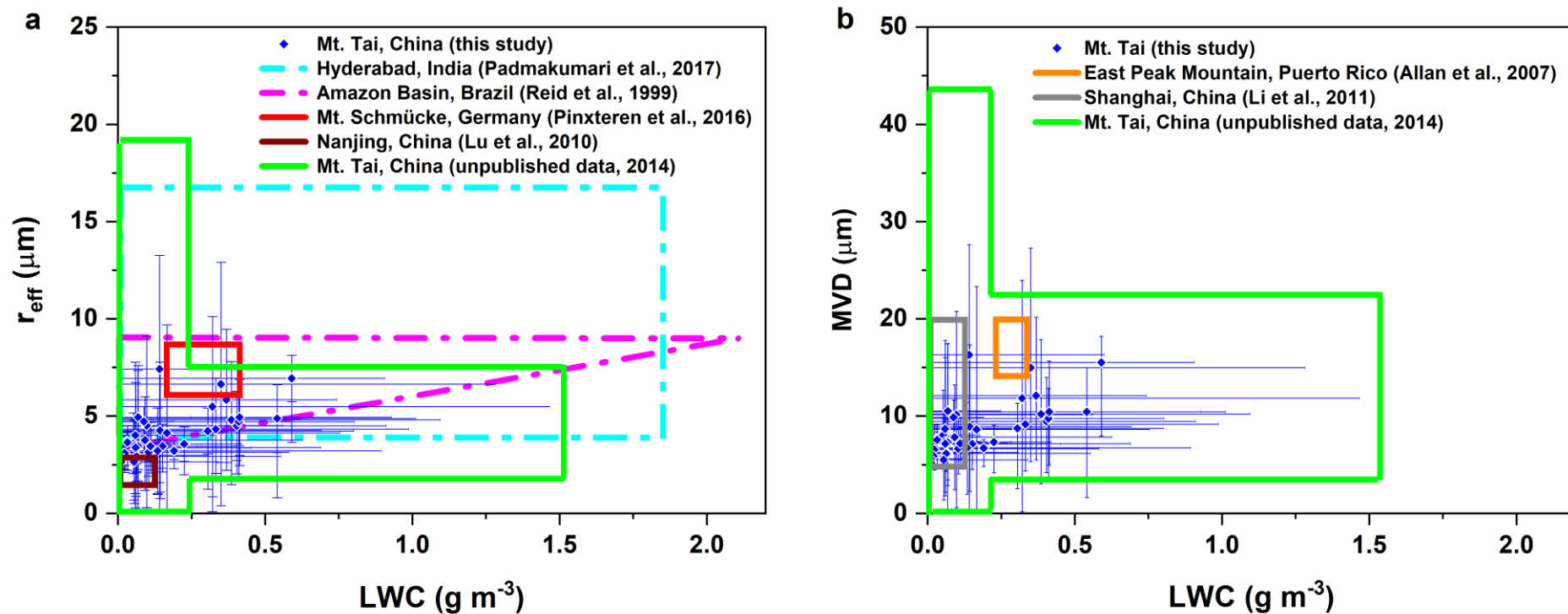


Figure 1: Plots of effective radius (r_{eff} , a) or medium volume diameter (MVD, b) against liquid water content (LWC) for clouds and fogs from the literatures. The dashed and solid shapes indicated the airborne and land observation, respectively. The blue diamonds with error bars represented the average LWC and r_{eff} (or MVD) of 40 cloud events observed at Mt. Tai in the present study with corresponding ranges

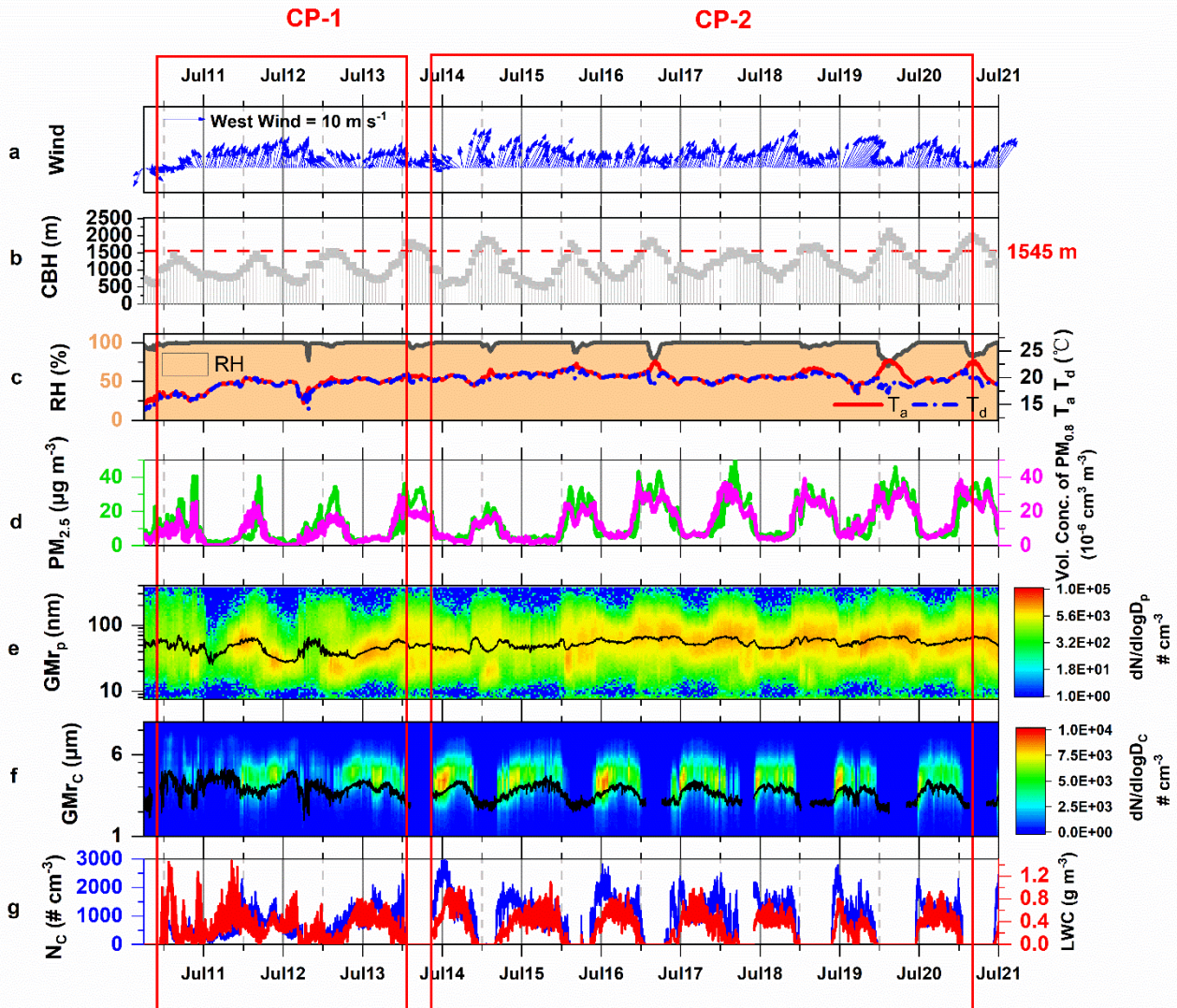


Figure 2: The monitoring information of CP-1 and CP-2. Including (a) Wind speed (WS, m s^{-1}) and wind direction (WD), (b) cloud based height (CBH, m) (c) relative humidity (RH, %), ambient temperature (T_a , $^{\circ}\text{C}$) and dew point temperature (T_d , $^{\circ}\text{C}$) (d) $\text{PM}_{2.5}$ mass concentrations ($\mu\text{g m}^{-3}$) and volumn concentration of $\text{PM}_{0.8}$ ($10^{-6} \text{ cm}^3 \text{ cm}^{-3}$) (e) size distribution of particles (13.6-763.5 nm) and corresponding geometric mean radius (GMr_p) (f) size distribution of cloud droplets (2-50 μm) and corresponding geometric mean radius (GMr_c) (g) N_c and LWC of cloud droplets.

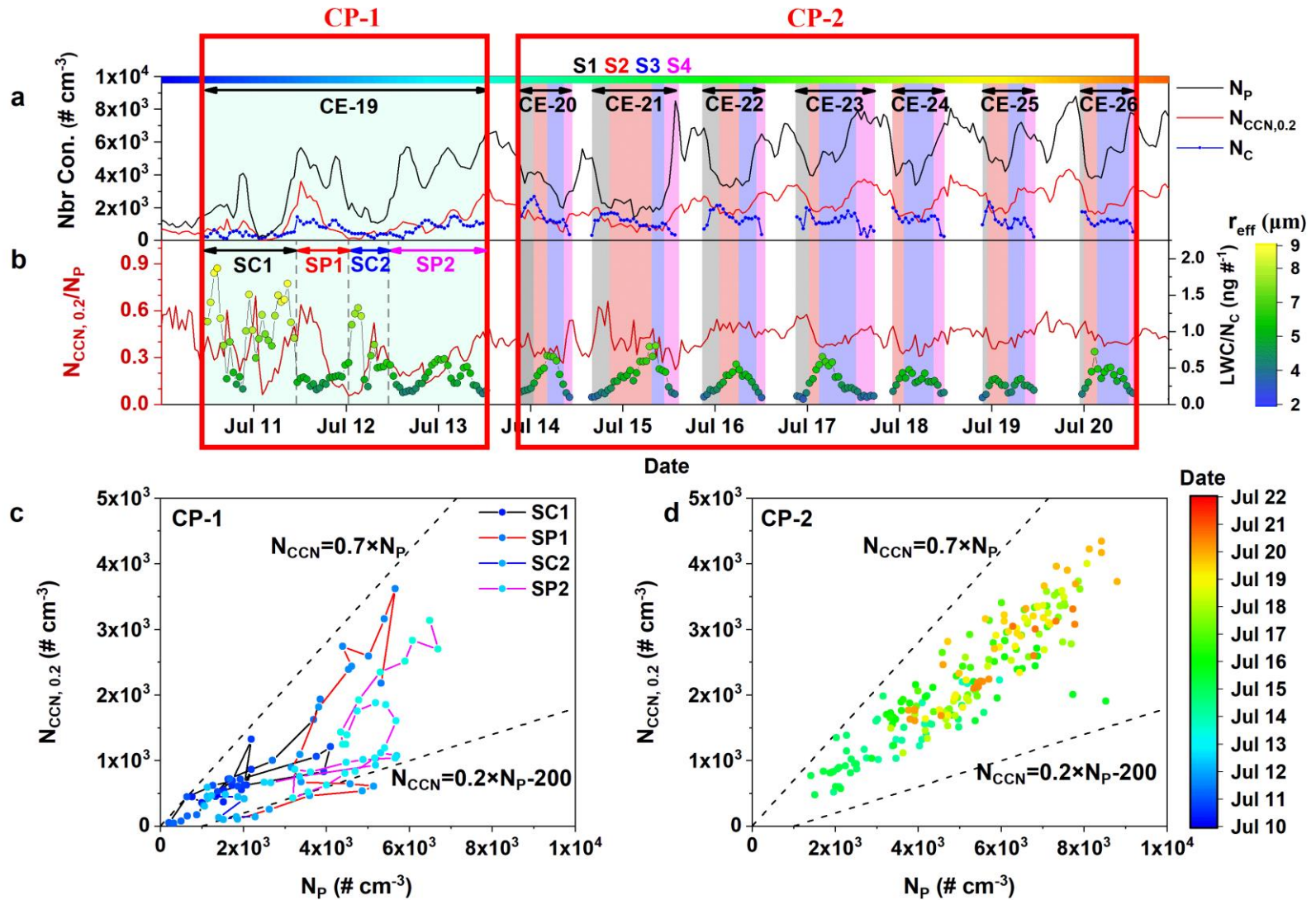


Figure 3: Variation of (a) N_c , N_p and $N_{CCN,0.2}$ (b) $N_{CCN,0.2}/N_p$ and LWC/N_c during CP-1 and CP-2. The plot of $N_{CCN,0.2}$ versus N_p (c) in CP-1 (d) in CP-2. The two dashed lines are the visually defined boundaries from the study of Asmi et al. (2012).

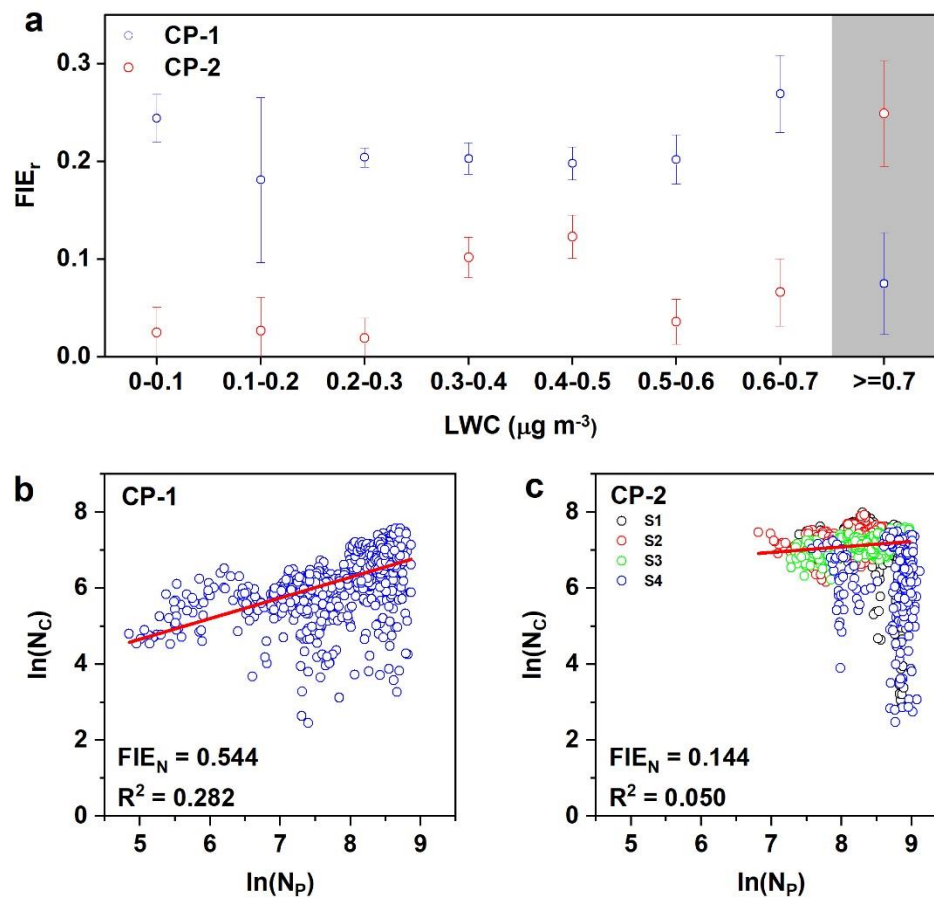


Figure 4: The determination of FIE (a) based on r_{eff} (b) and (c) based on N_C .

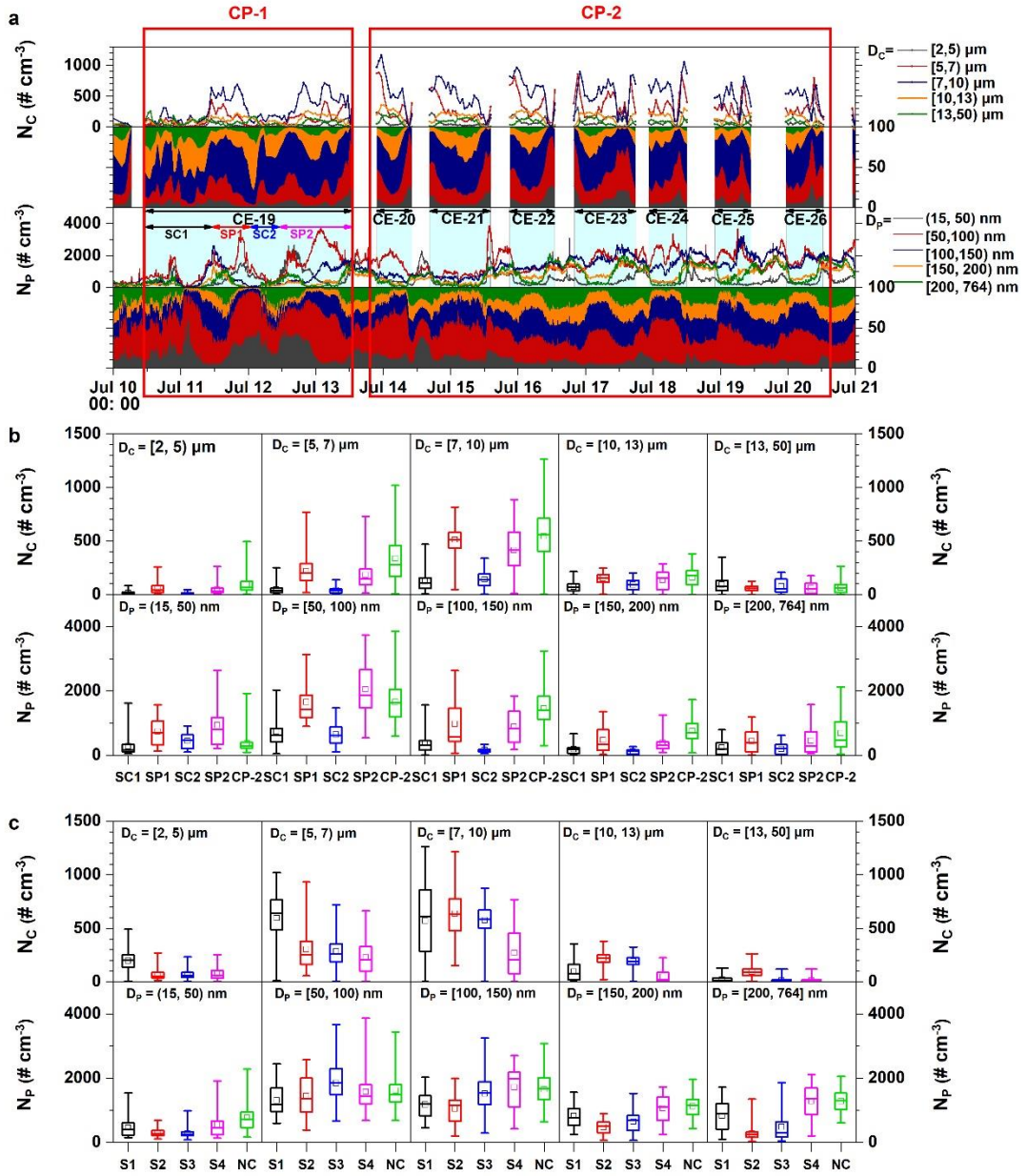


Figure 5: Size distribution of particles and cloud droplets during CP-1 and CP-2. (a) Time series plot of N_c in five size ranges ([2, 5] μm , [5, 7] μm , [7, 10] μm , [10, 13] μm and [13, 50] μm) and N_p in five size ranges ((15, 50) nm, [50, 100] nm, [100, 150] nm, [150, 200] nm, [200, 765] nm). (b) five size ranges of N_c and five size ranges of N_p in SC1, SP1, SC2, SP2 and CP-2 (c) five size ranges of N_c and five size ranges of N_p in S1, S2, S3, S4 and NC (“NC” in (c) represents particle size distributions during cloudless period).

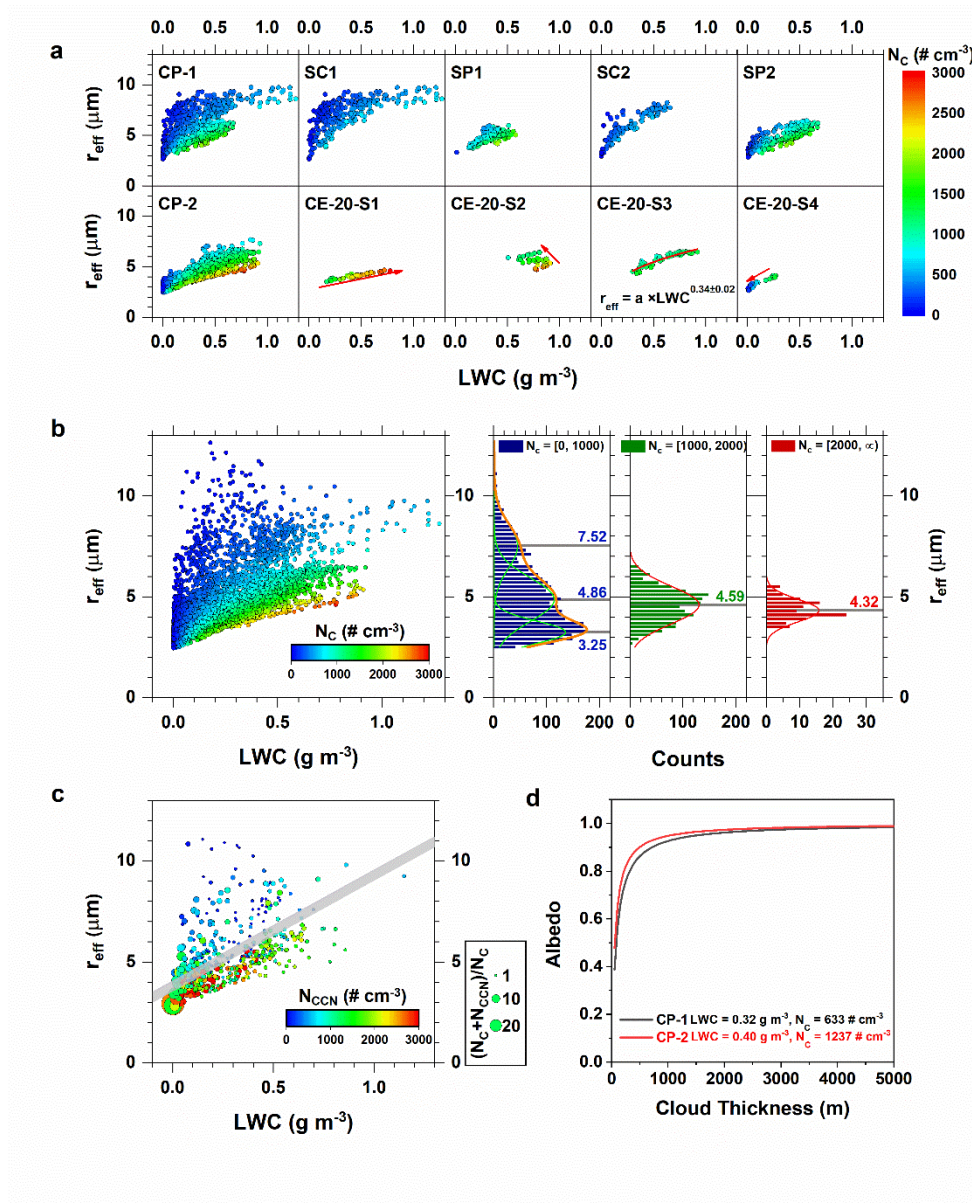


Figure 6: The plot of LWC versus r_{eff} (a) in different cloud stages of CP-1 and CP-2 (b) under different N_c ranges (c) under different N_{CCN} . The time resolution of the corresponding data was 5 min in (a), (b) and 50 min in (c). (d) The plot of albedo versus the variation of cloud thickness during CP-1 and CP-2. The averaged values of LWC and N_c of CP-1 and CP-2 were applied to calculate albedo according to the equations in Section 2.8.

Supplement Information

Table S1. Monitoring times of cloud events with averaged PM_{2.5} mass concentration, cloud droplet number concentration (N_C), mean liquid water content (LWC), effective radius (r_{eff}), geometrical mean diameter (GMD), droplet surface area (PSA), pressure (P), temperature (T), relative humidity (RH), wind direction (WD), wind speed (WS) and the number of cloud samples at Mt. Tai.

Event	Start	Stop	Duration	PM _{2.5}	N _C	LWC	r _{eff}	GMDc	PSA	P	T	RH	WD	WS	No.of Sample
	(UTC/GMT 8)	(UTC/GMT 8)	(h)	(μg m ⁻³)	(# cm ⁻³)	(g m ⁻³)	(μm)	(μm)	(cm ² m ⁻³)	(hPa)	(°C)	(%)	(°)	(m s ⁻¹)	(#)
1	2018/06/17 08:49	2018/06/17 09:08	0.3	34.48	156	0.03	3.9	6.8	234	84.4	14.9	90.8	203.6	1.3	0
2	2018/06/18 01:24	2018/06/18 03:02	1.6	23.23	202	0.02	3.3	5.7	268	84.2	13.3	98.8	241.1	4.1	0
3	2018/06/18 23:17	2018/06/19 00:05	0.8	44.18	300	0.06	4.1	6.4	469	84.0	14.7	97.3	233.3	3.1	0
4	2018/06/19 22:32	2018/06/19 23:26	0.9	87.65	385	0.05	3.7	5.6	478	84.3	16.0	97.8	95.0	1.9	0
5	2018/06/24 23:37	2018/06/25 22:14	22.6	7.92	558	0.35	6.8	9.4	1550	84.2	18.2	99.8	197.1	6.4	2
6	2018/06/27 23:31	2018/06/28 00:52	1.3	27.61	316	0.09	4.8	6.6	635	84.0	19.3	97.6	267.1	5.2	0
7	2018/07/01 22:40	2018/07/02 00:40	2.0	6.10	620	0.59	7.1	10.0	2481	84.2	16.6	99.2	93.4	4.2	1
8	2018/07/02 05:26	2018/07/02 08:15	2.8	31.00	402	0.06	3.6	5.9	484	84.2	16.2	98.9	58.8	3.3	0
9	2018/07/02 21:06	2018/07/02 22:02	0.9	66.02	240	0.02	3.0	4.9	230	84.1	16.4	98.5	90.7	3.0	0
10	2018/07/03 02:58	2018/07/03 06:31	3.6	41.65	380	0.07	4.0	5.9	719	83.9	15.8	97.6	34.2	4.6	0
11	2018/07/05 00:15	2018/07/05 06:25	6.2	46.44	730	0.11	3.8	5.6	1082	83.9	16.8	99.1	86.3	7.2	0
12	2018/07/05 21:35	2018/07/06 08:42	11.1	40.06	677	0.10	3.8	5.5	1137	84.2	17.4	98.8	73.2	8.6	1
13	2018/07/07 00:38	2018/07/07 02:00	1.4	28.18	462	0.06	3.6	5.4	606	84.4	16.1	98.7	98.6	4.8	0
14	2018/07/07 22:35	2018/07/08 03:00	4.4	14.68	193	0.06	5.1	6.8	456	84.4	15.9	99.8	203.6	4.8	1
15	2018/07/08 11:32	2018/07/08 22:30	11.0	20.01	440	0.14	4.9	7.2	963	84.5	16.0	97.4	89.9	5.7	2
16	2018/07/09 05:39	2018/07/09 12:18	6.6	2.99	59	0.14	9.8	12.4	525	84.5	16.0	99.6	72.6	5.8	0
17	2018/07/09 15:42	2018/07/09 22:14	6.5	11.14	166	0.07	5.3	6.6	625	84.5	15.8	93.5	92.9	2.4	0
18	2018/07/10 02:10	2018/07/10 04:55	2.7	8.17	121	0.10	6.9	8.1	627	84.5	15.5	95.6	207.1	3.4	0
19	2018/07/10 10:54	2018/07/13 12:51	74.0	8.71	633	0.32	6.0	8.4	1669	84.5	18.5	99.4	180.7	4.4	12
20	2018/07/13 21:17	2018/07/14 10:35	13.3	6.20	1519	0.54	5.2	7.5	3133	84.3	19.7	100.0	147.6	5.6	1
21	2018/07/14 15:58	2018/07/15 14:09	22.2	5.80	1081	0.39	5.2	7.6	2239	84.5	20.7	99.9	197.2	5.9	3

22	2018/07/15 20:42	2018/07/16 12:57	16.3	10.70	1346	0.40	4.9	7.1	2522	84.6	20.4	99.9	193.5	4.3	2
23	2018/07/16 20:43	2018/07/17 17:35	20.9	15.28	1147	0.33	4.9	6.8	2078	84.5	19.5	100.0	196.1	4.9	2
24	2018/07/17 22:07	2018/07/18 11:47	13.7	8.44	1250	0.41	4.9	7.5	2534	84.5	20.0	100.0	199.0	6.4	1
25	2018/07/18 21:36	2018/07/19 11:06	13.5	10.37	1161	0.31	4.6	6.9	2070	84.6	19.4	99.9	200.8	6.8	1
26	2018/07/19 22:51	2018/07/20 12:59	14.1	9.16	1157	0.41	5.2	7.5	2382	84.5	19.7	100.0	192.9	5.2	2
27	2018/07/20 22:27	2018/07/21 03:02	4.6	12.48	938	0.15	3.8	6.0	1237	84.5	18.7	99.8	210.9	6.4	1
28	2018/07/21 23:03	2018/07/21 23:36	0.6	21.02	607	0.06	3.2	5.5	622	84.6	18.4	98.9	199.4	7.1	0
29	2018/07/22 22:49	2018/07/22 23:34	0.8	7.22	1437	0.19	3.5	5.7	1658	84.4	18.6	99.2	81.3	9.7	0
30	2018/07/23 03:46	2018/07/23 18:29	14.7	1.87	630	0.37	6.0	9.8	1859	83.9	18.4	99.9	64.4	13.7	2
31	2018/07/24 09:03	2018/07/24 10:09	1.1	2.30	148	0.07	5.7	7.9	381	84.1	18.8	100.0	272.0	8.3	0
32	2018/07/24 11:34	2018/07/24 12:03	0.5	5.42	130	0.03	4.3	7.1	244	84.1	19.5	100.0	257.6	5.9	0
33	2018/07/24 18:20	2018/07/25 08:52	14.5	8.18	1441	0.23	3.7	6.1	1846	84.1	20.2	99.9	220.1	11.9	1
34	2018/07/25 19:29	2018/07/25 20:44	1.3	21.54	166	0.01	2.7	5.0	220	84.3	21.6	99.0	223.7	9.0	0
35	2018/07/26 01:38	2018/07/26 05:25	3.8	9.86	770	0.11	3.6	6.0	939	84.4	20.7	99.8	219.0	3.6	0
36	2018/07/26 19:32	2018/07/27 01:04	5.5	23.67	326	0.06	3.8	5.5	775	84.5	19.3	98.4	149.4	6.6	0
37	2018/07/27 12:17	2018/07/27 14:44	2.4	24.69	455	0.13	4.7	6.1	1185	84.5	20.0	94.5	89.9	4.5	0
38	2018/07/27 16:45	2018/07/30 00:05	55.3	10.68	445	0.17	5.1	7.3	1187	84.4	18.7	99.1	160.8	4.3	5
39	2018/07/30 03:55	2018/07/30 04:25	0.5	10.83	279	0.09	4.9	7.4	563	84.3	18.5	99.1	268.2	1.1	0
40	2018/07/30 06:29	2018/07/30 12:41	6.2	27.45	209	0.06	4.8	6.4	477	84.4	20.3	95.2	83.9	2.7	0

Table S2. Estimated updraft velocity (V_{up}) (means \pm S.D.), estimated cloud base height (CBH) (means \pm S.D.) and the sensitivities analysis of N_C to N_P , CBH and v_{up} during CP-1 and CP-2.

	V_{up} $m\ s^{-1}$	CBH m	^{a,b} $\partial \ln N_C / \partial \ln N_P (R^2)$	^b $\partial \ln N_C / \partial \ln CBH (R^2)$	^b $\partial \ln N_C / \partial \ln v_{up} (R^2)$
CP-1	1.31 \pm 0.46	1017.9 \pm 301.5	0.544(0.2820)	-0.118(0.0018)	0.275(0.0599)
CP-2	1.07 \pm 0.38	1040.4 \pm 260.2	0.144(0.0500)	0.216(0.1279)	0.515(0.0836)

^aThe value of $\partial \ln N_C / \partial \ln N_P$ was equal to FIE_N

^b R^2 represented correlation coefficient

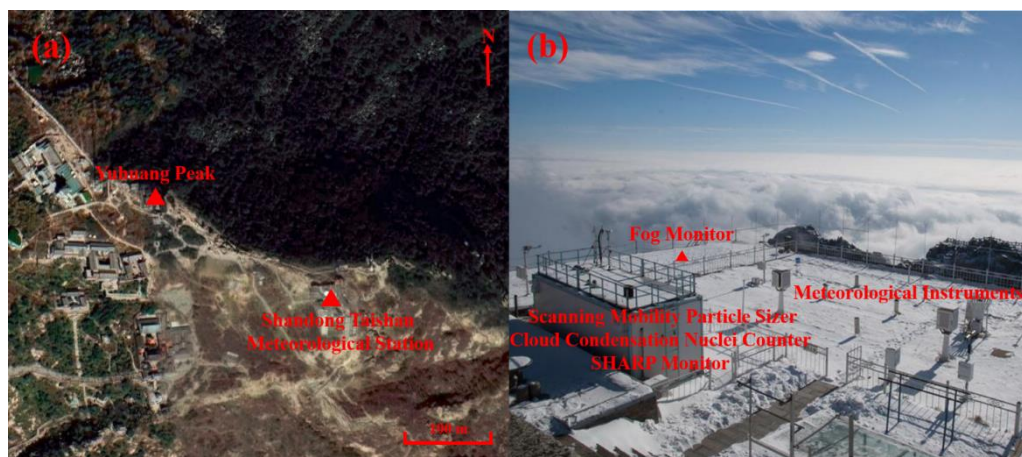


Figure S1. The pictures and schematic of (a) the measurement station (printscreen from Google Map) (b) the arrangement of instruments in Shandong Taishan Meteorological Station (<http://p.weather.com.cn/2016/12/2638460.shtml>). The corresponding sampling tubes were at least 1.5 m higher than the roof and at least 1.0 m away from each other to avoid the mutual interference.

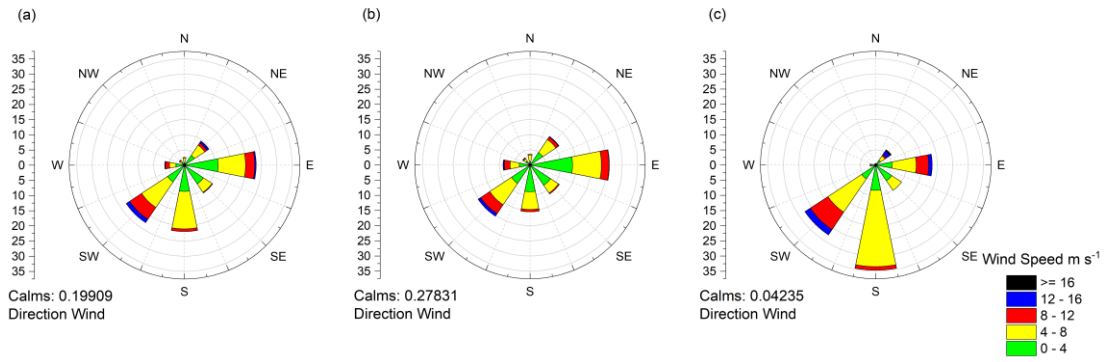


Figure S2. Wind direction and wind speed a) during the whole summer campaign at Mt. Tai, b) without cloud events and c) during cloud events.

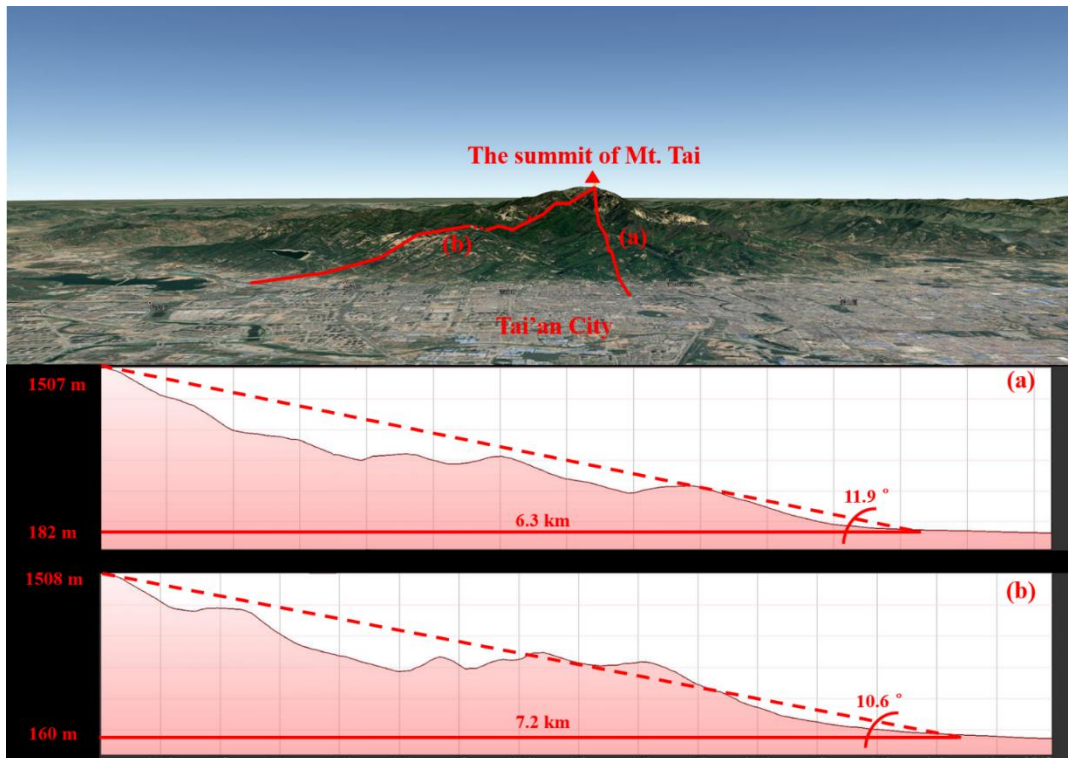


Figure S3. Influence of the topography on the vertical wind field at monitoring station. Taking (a) the south-north transect of Mt. Tai and (b) the southwest-northeast transect of Mt. Tai to estimate the inclination angles and updraft velocities.

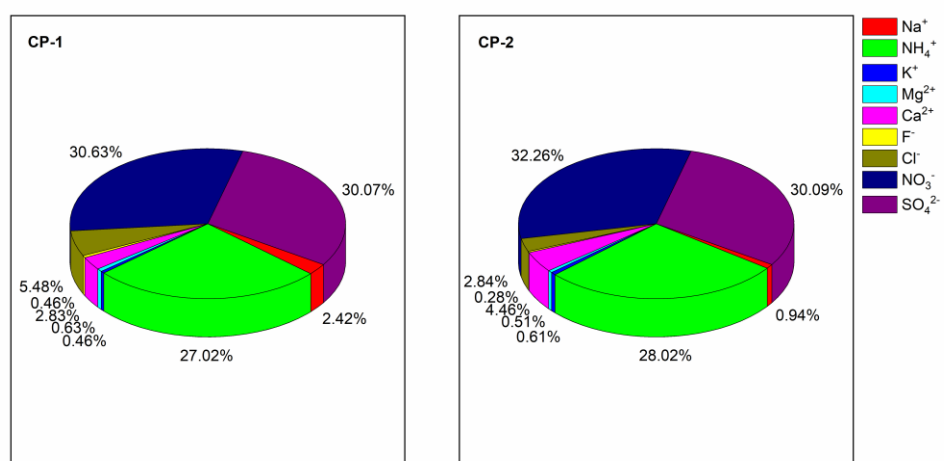


Figure S4. The averaged inorganic chemical compositions of cloud samples collected during CP-1 and CP-2. Each cloud process contained 12 cloud samples.

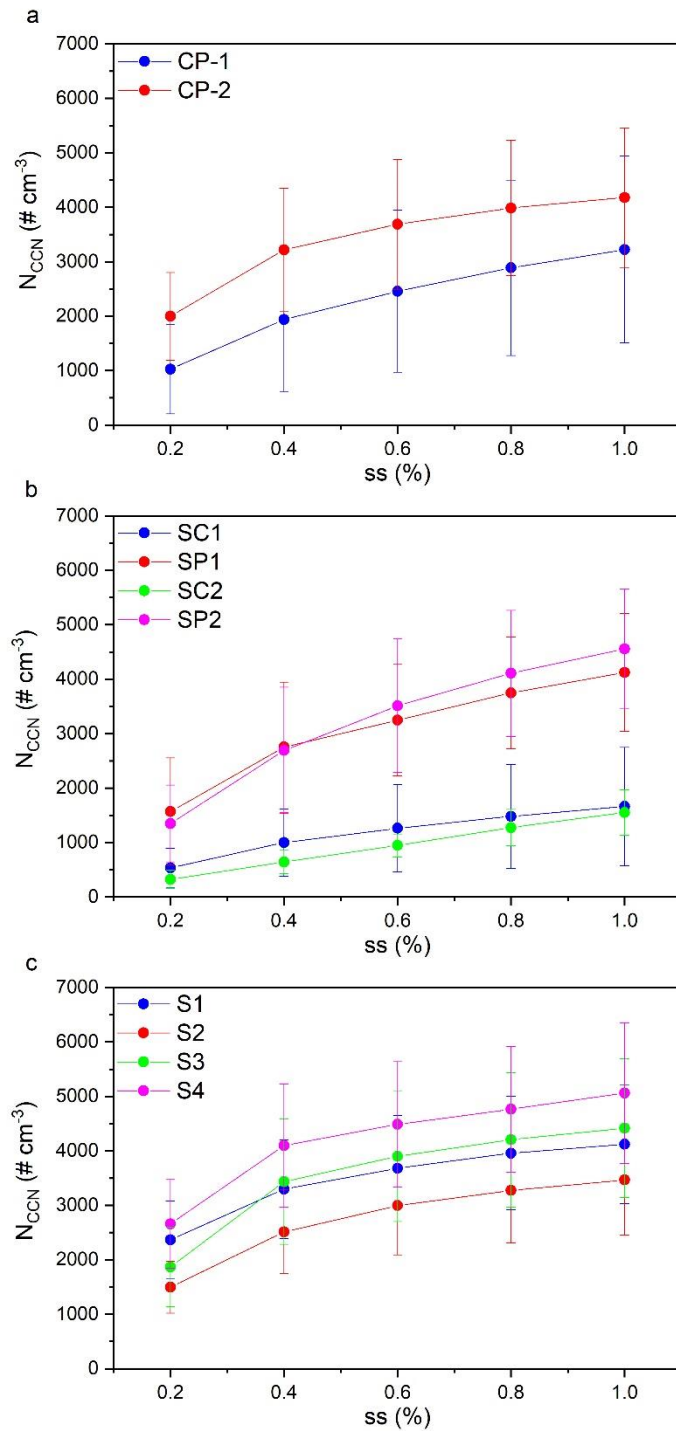


Figure S5: The N_{CCN} measured at $ss = 0.2\%$, 0.4% , 0.6% , 0.8% and 1.0% during (a) CP-1 and CP-2 (b) SC1, SP1, SC2 and SP2 (c) S1, S2, S3 and S4.

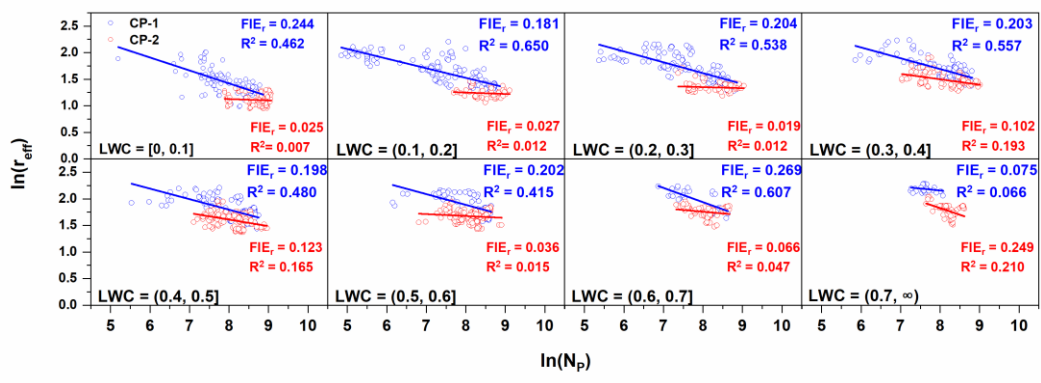


Figure S6: The calculation of FIE_r based on the plot of r_{eff} versus N_p in narrow LWC size bins with increase of 0.1 g m^{-3} .

Reference

- Ackerman, A. S., Kirkpatrick, M. P., Stevens, D. E., and Toon, O. B.: The impact of humidity above stratiform clouds on indirect aerosol climate forcing, *Nature*, 432, 1014-1017, 10.1038/nature03174, 2004.
- Asmi, E., Freney, E., Hervo, M., Picard, D., Rose, C., Colomb, A., and Sellegri, K.: Aerosol cloud activation in summer and winter at puy-de-Dome high altitude site in France, *Atmos. Chem. Phys.*, 12, 11589-11607, 10.5194/acp-12-11589-2012, 2012.
- Choulaton, T. W., Colvile, R. N., Bower, K. N., Gallagher, M. W., Wells, M., Beswick, K. M., Arends, B. G., Mols, J. J., Kos, G. P. A., Fuzzi, S., Lind, J. A., Orsi, G., Facchini, M. C., Laj, P., Gieray, R., Wieser, P., Engelhardt, T., Berner, A., Kruisz, C., Moller, D., Acker, K., Wiprecht, W., Luttke, J., Levens, K., Bizjak, M., Hansson, H. C., Cederfelt, S. I., Frank, G., Mentes, B., Martinsson, B., Orsini, D., Svenningsson, B., Swietlicki, E., Wiedensohler, A., Noone, K. J., Pahl, S., Winkler, P., Seyffer, E., Helas, G., Jaeschke, W., Georgii, H. W., Wobrock, W., Preiss, M., Maser, R., Schell, D., Dollard, G., Jones, B., Davies, T., Sedlak, D. L., David, M. M., Wendisch, M., Cape, J. N., Hargreaves, K. J., Sutton, M. A., StoretonWest, R. L., Fowler, D., Hallberg, A., Harrison, R. M., and Peak, J. D.: The Great Dun Fell Cloud Experiment 1993: An overview, *Atmospheric Environment*, 31, 2393-2405, 10.1016/s1352-2310(96)00316-0, 1997.
- Cross, E. S., Slowik, J. G., Davidovits, P., Allan, J. D., Worsnop, D. R., Jayne, J. T., Lewis †, D. K., Canagaratna, M., and Onasch, T. B.: Laboratory and Ambient Particle Density Determinations using Light Scattering in Conjunction with Aerosol Mass Spectrometry, *Aerosol Sci. Technol.*, 41, 343-359, 10.1080/02786820701199736, 2007.
- Demoz, B. B., Collett, J. L., and Daube, B. C.: On the Caltech Active Strand Cloudwater Collectors, *Atmos. Res.*, 41, 47-62, 10.1016/0169-8095(95)00044-5, 1996.
- Drewnick, F., Schneider, J., Hings, S. S., Hock, N., Noone, K., Targino, A., Weimer, S., and Borrmann, S.: Measurement of ambient, interstitial, and residual aerosol particles on a mountaintop site in central Sweden using an aerosol mass spectrometer and a CVI, *Journal of Atmospheric Chemistry*, 56, 1-20, 10.1007/s10874-006-9036-8, 2007.
- Durkee, P. A., Noone, K. J., Ferek, R. J., Johnson, D. W., Taylor, J. P., Garrett, T. J., Hobbs, P. V., Hudson, J. G., Bretherton, C. S., Innis, G., Frick, G. M., Hoppel, W. A., O'Dowd, C. D., Russell, L. M., Gasparovic, R., Nielsen, K. E., Tessmer, S. A., Ostrom, E., Osborne, S. R., Flagan, R. C., Seinfeld, J. H., and Rand, H.: The impact of ship-produced aerosols on the microstructure and albedo of warm marine stratocumulus clouds: A test of MAST hypotheses 1i and 1ii, *Journal of the Atmospheric Sciences*, 57, 2554-2569, 10.1175/1520-0469(2000)057<2554:Tiospa>2.0.Co;2, 2000.
- Freud, E., and Rosenfeld, D.: Linear relation between convective cloud drop number concentration and depth for rain initiation, *J. Geophys. Res.: Atmos.*, 117, 13, 10.1029/2011jd016457, 2012.
- Hammer, E., Bukowiecki, N., Gysel, M., Juranyi, Z., Hoyle, C. R., Vogt, R., Baltensperger, U., and Weingartner, E.: Investigation of the effective peak supersaturation for liquid-phase clouds at the high-alpine site Jungfraujoch, Switzerland (3580 m a.s.l.), *Atmospheric Chemistry and Physics*, 14, 1123-1139, 10.5194/acp-14-1123-2014, 2014.
- Heintzenberg, J., Ogren, J. A., Noone, K. J., and Gardneus, L.: The Size Distribution of Submicrometer Particles within and about Stratocumulus Cloud Droplets on Mt. Areskutan, Sweden, *Atmospheric Research*, 24, 89-101, 10.1016/0169-8095(89)90039-2, 1989.
- Li, S., Joseph, E., Min, Q., and Yin, B.: Multi-year ground-based observations of aerosol-cloud interactions in the Mid-Atlantic of the United States, *J. Quant. Spectrosc. Radiat. Transfer*, 188,

- 192-199, 10.1016/j.jqsrt.2016.02.004, 2017b.
- Mazoyer, M., Burnet, F., Denjean, C., Roberts, G. C., Haeffelin, M., Dupont, J. C., and Elias, T.: Experimental study of the aerosol impact on fog microphysics, *Atmos. Chem. Phys.*, 19, 4323-4344, 10.5194/acp-19-4323-2019, 2019.
- Mertes, S., Galgon, D., Schwirn, K., Nowak, A., Lehmann, K., Massling, A., Wiedensohler, A., and Wieprecht, W.: Evolution of particle concentration and size distribution observed upwind, inside and downwind hill cap clouds at connected flow conditions during FEBUKO, *Atmos. Environ.*, 39, 4233-4245, 10.1016/j.atmosenv.2005.02.009, 2005.
- Modini, R. L., Frossard, A. A., Ahlm, L., Russell, L. M., Corrigan, C. E., Roberts, G. C., Hawkins, L. N., Schroder, J. C., Bertram, A. K., Zhao, R., Lee, A. K. Y., Abbatt, J. P. D., Lin, J., Nenes, A., Wang, Z., Wonaschuetz, A., Sorooshian, A., Noone, K. J., Jonsson, H., Seinfeld, J. H., Toom-Sauntry, D., Macdonald, A. M., and Leitch, W. R.: Primary marine aerosol-cloud interactions off the coast of California, *Journal of Geophysical Research-Atmospheres*, 120, 4282-4303, 10.1002/2014jd022963, 2015.
- Noone, K. J., Ogren, J. A., and Heintzenberg, J.: An Examination of Clouds at a Mountain-Top Site in Central Sweden: The Distribution of Solute within Cloud Droplets, *Atmospheric Research*, 25, 3-15, 10.1016/0169-8095(90)90002-t, 1990.
- Platnick, S., Durkee, P. A., Nielsen, K., Taylor, J. P., Tsay, S. C., King, M. D., Ferek, R. J., Hobbs, P. V., and Rottman, J. W.: The role of background cloud microphysics in the radiative formation of ship tracks, *Journal of the Atmospheric Sciences*, 57, 2607-2624, 10.1175/1520-0469(2000)057<2607:Trobcm>2.0.Co;2, 2000.
- Qian, Y., Gong, D. Y., Fan, J. W., Leung, L. R., Bennartz, R., Chen, D. L., and Wang, W. G.: Heavy pollution suppresses light rain in China: Observations and modeling, *J. Geophys. Res.: Atmos.*, 114, 16, 10.1029/2008jd011575, 2009.
- Rosenfeld, D., Andreae, M. O., Asmi, A., Chin, M., de Leeuw, G., Donovan, D. P., Kahn, R., Kinne, S., Kivekas, N., Kulmala, M., Lau, W., Schmidt, K. S., Suni, T., Wagner, T., Wild, M., and Quaas, J.: Global observations of aerosol-cloud-precipitation-climate interactions, *Rev. Geophys.*, 52, 750-808, 10.1002/2013rg000441, 2014a.
- Roth, A., Schneider, J., Klimach, T., Mertes, S., van Pinxteren, D., Herrmann, H., and Borrmann, S.: Aerosol properties, source identification, and cloud processing in orographic clouds measured by single particle mass spectrometry on a central European mountain site during HCCT-2010, *Atmos. Chem. Phys.*, 16, 505-524, 10.5194/acp-16-505-2016, 2016.
- Schroder, J. C., Hanna, S. J., Modini, R. L., Corrigan, A. L., Kreidenwies, S. M., Macdonald, A. M., Noone, K. J., Russell, L. M., Leitch, W. R., and Bertram, A. K.: Size-resolved observations of refractory black carbon particles in cloud droplets at a marine boundary layer site, *Atmospheric Chemistry and Physics*, 15, 1367-1383, 10.5194/acp-15-1367-2015, 2015.
- Spiegel, J. K., Zieger, P., Bukowiecki, N., Hammer, E., Weingartner, E., and Eugster, W.: Evaluating the capabilities and uncertainties of droplet measurements for the fog droplet spectrometer (FM-100), *Atmospheric Measurement Techniques*, 5, 2237-2260, 10.5194/amt-5-2237-2012, 2012.
- Targino, A. C., Noone, K. J., Drewnick, F., Schneider, J., Krejci, R., Olivares, G., Hings, S., and Borrmann, S.: Microphysical and chemical characteristics of cloud droplet residuals and interstitial particles in continental stratocumulus clouds, *Atmospheric Research*, 86, 225-240, 10.1016/j.atmosres.2007.05.001, 2007.
- Twohy, C. H., Petters, M. D., Snider, J. R., Stevens, B., Tahnk, W., Wetzal, M., Russell, L., and Burnet,

- F.: Evaluation of the aerosol indirect effect in marine stratocumulus clouds: Droplet number, size, liquid water path, and radiative impact, *J. Geophys. Res.: Atmos.*, 110, -, 2005.
- Twomey, S.: Pollution and planetary albedo, *Atmos. Environ.*, 8, 1251-1256, 10.1016/0004-6981(74)90004-3, 1974.
- Twomey, S. A.: The Influence of Pollution on the Shortwave Albedo of Clouds, *J. Atmos. Sci.*, 34, 1149-1154, 1977.
- Verheggen, B., Cozic, J., Weingartner, E., Bower, K., Mertes, S., Connolly, P., Gallagher, M., Flynn, M., Choulaton, T., and Baltensperger, U.: Aerosol partitioning between the interstitial and the condensed phase in mixed-phase clouds, *Journal of Geophysical Research-Atmospheres*, 112, 13, 10.1029/2007jd008714, 2007.
- Welch, R. M., Asefi, S., Zeng, J., Nair, U. S., Han, Q., Lawton, R. O., Ray, D. K., and Manoharan, V. S.: Biogeography of tropical montane cloud forests. Part I: Remote sensing of cloud-base heights, *Journal of Applied Meteorology and Climatology*, 47, 960-975, 10.1175/2007jamc1668.1, 2008.
- Yuan, T., Li, Z., Zhang, R., and Fan, J.: Increase of cloud droplet size with aerosol optical depth: An observation and modeling study, *J. Geophys. Res.: Atmos.*, 113, 10.1029/2007jd008632, 2008.